

Recombinant Human Endostatin against the development of RIPF in a murine model

HANG JIE YING

Institute of cancer research and basic medical science of chinese academy of science

CHENG ZHOU

Institute of cancer research and basic medical science of chinese academy of science

MEI YA CHEN

Institute of cancer research and basic medical science of chinese academy of science

YUAN MENG CHEN

zhejiang key laboratory of radiation oncology

QIANG BAI DONG

Institute of cancer research and basic medical science of chinese academy of science

MIN FANG (✉ fangmin@zjcc.org.cn)

Department of radiation oncology <https://orcid.org/0000-0003-1476-3116>

MING CHEN

Institute of cancer research and basic medical science of chinese academy of science

Research article

Keywords: Endostar; Radiation; Lung; Fibrosis; Angiogenesis

Posted Date: July 28th, 2019

DOI: <https://doi.org/10.21203/rs.2.11995/v1>

License:  This work is licensed under a Creative Commons Attribution 4.0 International License.

[Read Full License](#)

Abstract

Abstract Background: Recent evidence has demonstrated the role of angiogenesis in the pathogenesis of pulmonary fibrosis. This study aimed to assess the therapeutic effect of Recombinant Human Endostatin (Endostar) administration on histopathological markers of radiation-induced pulmonary fibrosis, and investigate the underlying mechanism. **Methods:** 80 Inbred C57BL/6 female mice were randomly divided into four treatment groups: No treatment group (NT, normal saline control), Radiation treatment group (RT), Endostar treatment group (EN), Endostar plus radiation treatment group (RT+EN). RT and RT+EN mice were exposed to a single-fraction 16Gy of 6MV X-ray for thorax irradiation. Mice in EN and RT+EN groups were given a daily subcutaneous injection of Endostar at a dose of 20 mg/kg, and thorax irradiation was performed 3 days after the first subcutaneous injection. Mice were sacrificed at 12 and 24 weeks post-irradiation. Pulmonary tissue was used in hematoxylin-eosin (H&E) and Masson's trichrome staining, as well as for immunohistochemical assessment of CD31, Collagen I and Collagen IV, and reverse transcription-polymerase chain reaction (RT-PCR) was used to detect the expression level of vascular endothelial growth factor (VEGF) and transforming growth factor- β 1 (TGF- β 1). The protein expression level of TGF- β 1, α -smooth muscle actin (α -SMA), total drosophila mothers against decapentaplegic protein 3 (Smad3), phosphorylate Smad3 (p-Smad3), total extracellular signal-regulated kinase (ERK) and phosphorylate ERK (p-ERK), β -Actin were analyzed by western blot. **Results:** During the observation period, the hair of irradiated groups showed whitening in the irradiated area and radiation induced body weight loss of mice was partially attenuated by Endostar treatment. Endostar treatment significantly reduced alveolar inflammation and pulmonary fibrosis in RT+EN group compared with RT group, as indicated by a decrease in the expression level of Collagen I, Collagen IV and CD31 in lung tissue. Thorax irradiation significantly increased the expression of TGF- β 1 and VEGF mRNA as well as α -SMA, TGF- β 1, p-Smad3, p-ERK protein in lung tissue of mice, however, those were attenuated after Endostar treatment. **Conclusion:** Endostar could reduce radiation-induced pulmonary fibrosis in mice, and this effect may be related to the inhibition of angiogenesis and TGF- β 1/Smad3/ERK pathway.

1. Background

Radiation therapy is an important treatment strategy for thoracic cancers. However, radiation-induced lung injury (RILI) is a common complication from the radiotherapy treatment of lung cancer, esophageal cancer and other mediastinal tumors, such as lymphoma and thymoma [1]. Clinical data have demonstrated that the incidence of RILI ranges from 5% to 30%. It is an important factor affecting the prognosis and quality of life for patients. The risk of RILI can be further increased as radiotherapy is always combined with chemotherapy drugs such as bleomycin, cisplatin, etoposide, 5-fluorouracil and paclitaxel for lung cancer treatment [2]. RILI includes two phases, acute phase of pneumonitis and late/chronic stage of fibrosis [3]. At present, glucocorticoids are used mainly in clinical treatment for early radiation pneumonitis. Radiation-induced pulmonary fibrosis (RIPF) will lead to progressively worsen alveolar structural disorders and irreversible lung fiber tissue remodeling, eventually leading to respiratory

failure, and currently there is no any effective treatment [4]. Thus, it is of great urgency to develop novel compounds to alleviate RIPP.

With the development of molecular and cellular biology, the role of angiogenesis in pulmonary fibrosis has been paid more and more attention. Angiogenesis may be a key factor in the development of pulmonary fibrosis [5-6]. In 1963, Turner-Warrick et al.[7] found an increase in the formation and remodeling of neovascularization in the lungs of patients with idiopathic pulmonary fibrosis (IPF), and an increase in microvessels in the pulmonary fibrosis area at autopsy. Then, many studies have demonstrated that the inhibition of angiogenesis attenuates pulmonary fibrosis in various animal models [8-10].

Endostatin, a 20 kDa C-terminal fragment of collagen XVIII, has been studied as a broad-spectrum and low toxicity multitarget angiogenesis inhibitor since being isolated from a murine hemangi endothelioma in 1997 [11]. O'Reilly et al[12] demonstrated that systemically administered Endostatin inhibited the growth of Lewis lung metastases and could also inhibit a number of primary tumors including Lewis lung, T241 fibrosarcomas, and B16F10 melanomas. With the deepening of research, Endostatin may inhibit tumor growth up to 65 different tumor types [13]. However, the anti-tumor effects of Endostatin were yet to be demonstrated in phase II clinical trials [14-15]. Recombinant Human Endostatin (Endostar) is a novel Endostatin with an additional nine-amino acid sequence forming his-tag structure, which not only improves its stability, prolongs half-life, but also increases biological activities [16]. The purity of Endostar is more than 99.9%, which is much higher than Endostatin, and it is at least twice as potent as Endostatin in animal tumor models [17]. Phase II and phase III clinical studies revealed that Endostar combined with vinorelbine platinum (NP) therapy for advanced non-small cell lung cancer (NSCLC) could significantly improve the effective rate and median tumor progression time [18-21]. In 2005, Endostar was approved by the China's State Food and Drug Administration (SFAD) for the treatment of NSCLC [22].

Wan et al. [23] found that Endostatin could reduce bleomycin-induced IPF in rats by inhibiting the expression of VEGF and ERK pathways. Yamaguchi et al. [24] reported that carboxyl-terminal polypeptides extracted and derived from Endostatin could significantly reduce IPF induced by TGF- β or bleomycin in mice. It was reported that Endostatin was significantly elevated in both bronchoalveolar lavage fluid (BALF) and plasma of IPF patients compared with controls, and Endostatin could inhibit distal lung epithelial cell (DLEC) wound repair. These suggested that Endostatin may play a role in aberrant epithelial repair in IPF [25].

The pathological characteristics of IPF are very similar to those of RIPP. The most sensitive subunit to ionizing radiation is the alveolar-capillary barrier (ACB). ACB is mainly composed of vascular endothelial cells and alveolar epithelial cells. The damage to alveolar epithelial cells and vascular endothelial cells results in secretion of a large number of cytokines, such as interleukins (IL-6, IL-8, IL-4, IL-1 β), tumor necrosis factor- α (TNF- α), monocyte chemotactic protein-1 (MCP-1), TGF- β , platelet-derived growth factor (PDGF) and basic fibroblast growth factor (bFGF) which were involved in local injury and inflammatory response and could lead to accumulation of fibroblasts that results in lung fibrosis. More importantly,

cytokines produced in this process will continue to trigger the activation of other cells resulting in cytokines cascade reactions [26]. Endostar has been reported to attenuate RILI of mice by inhibiting the expression of TGF- β 1, but the deeper mechanisms have not been elucidated [27].

Therefore, this study aims to constructing the mouse RIPF model, so as to better explore the therapeutic effects of Endostar on RIPF and elucidate the underlying mechanisms.

2. Methods

2.1 Animals and Agents

10-12 weeks old inbred C57BL/6 female mice (body weight 18-20g) were provided by Shanghai Xipuer Bikai Experimental Animal Co., Ltd. (production license: SCXK 2013-0016, Shanghai, China) and raised in the SPF animal breeding room of Experimental Animal Center of Zhejiang Chinese Medical University (Hangzhou, China), housed six per cage under standard laboratory conditions and had free access to food and water. The mice go in and out of the SPF animal room by using dedicated sealed transfer boxes with air filtration. Endostar (15mg/3ml; Shandong Simcere-Medgenn Bio-Pharmaceutical Co., Ltd. Yantai, China.), and normal saline as a vehicle.

2.2 Irradiation and Endostar Treatment

After one week of acclimation in the room, 80 female C57BL/6 mice were randomized into 4 groups: no treatment group (NT, normal saline), radiation alone group (RT), Endostar alone group (EN), and Endostar plus radiation group (RT+EN). For radiation exposure, mice were anesthetized using pentobarbital sodium (40mg/kg, intraperitoneally) and received a single whole lung X-ray consisting of a 16Gy dose of radiation by using Varian's Trilogy Tx medical linear (6MV; 600cGy/min; SSD=100cm; Varian Medical Systems Inc. USA). For Endostar administration, 20mg/kg/d of Endostar was administrated subcutaneous injection 3 days before irradiation for 12 or 24 weeks [28-29].

2.3 Histology

Mice were fixed on the operating table and killed by femoral artery bleeding at 12 or 24 weeks post-irradiation, each procedure was performed under sodium pentobarbital anesthesia (40mg/kg, intraperitoneally), and all efforts were made to minimize suffering. The right lungs were stored at -80°C for qRT-PCR and Western blot analysis, and the left lungs were fixed in 4% paraformaldehyde, dehydrated, and embedded in paraffin. The tissues were then sectioned at 5 μ m and stained with H&E, Masson's trichrome to examine the degree of fibrosis. Ten fields in each section were analyzed. The severity of fibrotic changes in each histological section of the lung was assessed as the mean score of severity from the observed microscopic fields using the semi-quantitative grading system described by Ashcroft and co-workers [30].

After deparaffinization in xylene, hydration with graded alcohol and subjected to antigen retrieval, the tissue sections were placed in 3% hydrogen peroxide (H₂O₂) for 10 minutes at room temperature to inactivate endogenous peroxidases. After washing three times in PBS, the slides were blocked with 2% bovine serum albumin (BSA) for 30 minutes at room temperature, followed by incubation with primary antibodies against the CD31 (1:200, ab28364, Abcam, Cambridge, UK), Collagen I (1:200, ab34710, Abcam, Cambridge, UK) and Collagen IV (1:200, ab6586, Abcam, Cambridge, UK) at 4°C overnight. After washing with PBS, the slides were incubated with secondary antibody (1:200, ab150077, Abcam, Cambridge, UK) for 60 minutes at 37°C. The slides then were washed in PBS for three times, followed by the DAB detection and counterstaining with haematoxylin.

For immunohistochemistry (IHC) scoring, positive reactions were defined as those showing brown signals, five fields were randomly selected and observed under a light microscope. The intensity was scored as follows: 0, negative; 1, weak; 2, moderate; and 3, strong. The frequency of positive cells was defined as follows: 0, less than 5%; 1, 5% to 25%; 2, 26% to 50%; 3, 51% to 75%; and 4, greater than 75%. IHC total score was calculated as the product of both scores. After whole section examination, IHC score was calculated as the mean score of all the fields.

2.4 Real-time PCR

Total RNA was extracted with TRIzol reagent (Takara Bio Inc. Japan), qRT-PCR was performed with SYBR®Premix Ex Taq II (Takara Bio Inc. Japan) after reverse transcribing 1µg of RNA with PrimeScript™RT Master Mix (Takara Bio Inc. Japan). qRT-PCR of the resulting cDNA was performed in triplicate with gene specific primers on ABI-7500 system (Applied Biosystems, USA). Levels were normalized to β-Actin with the 2^{-ΔΔCt} method and relative to control samples. The primers for qRT-PCR are listed in Table 1.2.6 Statistical Analyses

2.5 Western blot

Protein samples (40 µg) were mixed with SDS-PAGE loading buffer, boiled at 100°C for 5 minutes. After electrophoresis, the proteins were transferred to PVDF membrane filters (Millipore Biotechnology Inc., USA). The membrane was blocked with 5% BSA for 60 minutes at room temperature. The membrane was incubated with the primary antibodies against the TGF-β1(1:1000, ab92486, Abcam, Cambridge, UK), α-SMA (1:1000, ab32575, Abcam, Cambridge, UK), p-Smad3(1:1000, ab52903, Abcam, Cambridge, UK), Smad3(1:1000,ab40854, Abcam, Cambridge, UK), ERK (1:1000,137F5, Cell Signaling Technology, Inc, USA) and p-ERK (1:1000, ab201015, Abcam, Cambridge, UK), β-Actin (1:5000, A2228, Sigma, Japan) in 5% BSA overnight at 4°C, washed three times with TBST for 5 minutes each time at room temperature, and then incubated with secondary antibodies (1:5000, ab150077, Abcam, Cambridge, UK or 1:5000, ab150113, Abcam, Cambridge, UK) for 60 minutes at room temperature. After three additional washes with TBST, the immune-reactive bands were visualized with enhanced chemiluminescent reagent (ECL, Millipore Biotechnology Inc., USA) and quantified by Multi Gauge V3.2 (Fuji Film, Japan) analysis software.

2.6 Statistical Analyses

Each experiment was repeated three times and data was recorded and analyzed with Prism 6.0 software. A one-way analysis of variance (ANOVA) was used to test the hypotheses and results with a P-value <0.05 considered statistically significant.

3. Results

3.1 Physical Status

During the 24 weeks observation period, 1 and 2 mice died in RT group at the 20th and 24th week, respectively. Six weeks post-irradiation, there was obvious hair whitening in the irradiated area of mice from RT and RT+EN groups (Fig.1A). Body weights of mice were monitored as a general measure of clinical status (Fig1.B). Single dose of 16 Gy to the chest obviously reduces the body weight of mice, whereas this radiation induced side effect was partially attenuated by Endostar treatment from week 12 to the end of observation. As expected, Endostar treatment alone did not alter mouse's body weight.

3.2 Histopathological changes in lung tissue

(1) HE staining results

In NT and EN treatment groups, the alveolar walls were thin, the capillary walls were intact without bleeding, with clear structure, and no inflammatory changes were observed. At the 12th week post-irradiation, the alveolar walls of mice in RT group were moderately thickened, the alveolar cavity became smaller, and inflammatory cells were observed to have infiltrated the pulmonary interstitium. At the 24th week post-irradiation, the alveolar walls were significantly thicker than those in NT group, the alveolar cavity became significantly smaller, with exudative inflammatory changes observed accompanied by infiltration of inflammatory cells, thickening of the alveolar septum and destruction of alveolar structure. Fibroblasts were abundant, and focal fibrosis appeared in the perivascular, interstitial, atelectasis and surrounding areas. In RT+EN group, the lung tissue showed scattered infiltration of inflammatory cells in the interstitial tissue, however, the histological changes at each time point were significantly less than those in RT group (Fig.2A). The assessment of pneumonitis/alveolitis scores further confirmed that a reduction of pneumonitis/alveolitis in RT+EN group. (Fig.2B)

- **Masson's trichrome staining results**

In NT and EN groups, the lung tissue fibers exhibited thin and light staining; the alveolar walls were fine, and the lung tissue structures were normal. At 12 and 24 weeks post-irradiation, local fibrosis was observed in lung tissue from RT group, suggesting the formation of pulmonary fibrosis. The degree of local fibrosis in RT+EN group was significantly lower than that in RT group (Fig.3A). The assessment of pulmonary fibrosis scores further confirmed the reduction of fibrosis in RT+EN group (Fig. 3B).

3.3 Endostar reduced collagen deposition and **angiogenesis** in lung tissue with R1PF

In order to explore the impact of Endostar on angiogenesis and profibrotic cytokines, the expression of CD31 (angiogenesis marker), Collagen I and Collagen IV were analyzed by IHC. The expression levels of these three proteins were significantly higher in lung tissue from RT group than those from NT and EN groups. Collagen I and Collagen IV staining were broadly positive in fibrous interstitium in RT group. On the contrary, the amount of CD31, Collagen I and Collagen IV in the bronchi and alveoli were reduced in RT+EN group compared with RT group. As expected, CD31, Collagen I and Collagen IV expression were negligible in the lung tissues of NT and EN group (Fig.4 A &B).

3.4. Endostar decreased TGF- β 1, VEGF mRNA expression and suppressed myofibroblasts (MFBs) activation by inhibiting TGF- β 1/Smad3/ERK pathway in lung tissue of mice after radiation.

To further evaluate the mechanism of the radioprotective effect of Endostar, the expression of TGF- β 1 and VEGF mRNA by RT-PCR, α -SMA, TGF- β 1, p-Smad3, Smad3, p-ERK, ERK, β -Actin were assessed by western blot. TGF- β 1 and VEGF mRNA levels was up-regulated in RT group, which were partially reversed by the treatment of Endostar (Fig. 5A). Western blot analysis demonstrated that the expression of α -SMA, TGF- β 1, p-Smad3, p-ERK increased significantly in RT group, and this expression was reduced in RT+EN group (Fig.5.B&C). These findings indicate that Endostar mitigates radiation-induced fibrosis by suppressing angiogenesis and TGF- β 1/Smad3/ERK signaling pathway.

Discussion

In the past ten years, despite the great development of large-scale precision radiotherapy equipments and medical imaging technology, the side effects caused by radiotherapy are still inevitable. RILI is a common complication in patients with lung cancer and other thoracic cancers after radiotherapy, and the precise pathogenic mechanisms remain unknown. Emerging evidence has demonstrated that angiogenesis is important in the development and progression of pulmonary fibrosis [31]. In order to confirm the effect of Endostar, which was independently developed by our country scholars of targeting angiogenesis to drug treatment, the RIPF model of C57BL/6 mice was induced by 16 Gy thorax irradiation with medical accelerator. In the present study, we demonstrated that Endostar treatment had the following effects: (1) decreasing collagen deposition; (2) reducing the expression of TGF- β 1 and VEGF mRNA; (3) inhibiting MFBs activation by suppressing TGF- β 1/Smad3/ERK signaling pathway. From these findings, we conclude that Endostar may play an important role in the course of pulmonary fibrosis induced by radiation, which may be mediated through its potentially regulatory effects on inhibiting angiogenesis and TGF- β 1/Smad3/ERK pathway.

Endostar is a novel modified Endostatin with an additional nine amino acids purified from *Escherichia coli* [11], which has a synergic activity and good safety without increasing side effects of chemotherapy[32]. In our study, 20mg/kg/d hypodermic injected Endostar had no influence on physical status of mice, suggesting that Endostar is generally safe and tolerable.

As previous studies showed that pretreatment of Endostatin could inhibit the fibrosis of human skin fibroblast and its transformation into MFBs[33]. Systemic administration of Endostatin could inhibit the

rabbit ear local hypertrophic scar formation[34]. Parenteral or intratracheal administration of a peptide derived from Endostatin could prevent and ameliorate fibrosis in a bleomycin-induced pulmonary fibrosis model[35]. These studies indicated that Endostatin had an anti-fibrotic effect and might have therapeutic potential to prevent or reverse organ fibrosis which were similar to our findings. Our study found that radiation-stressed mice were featured by the body weight loss, lung tissue alveolitis and fibrosis. After subcutaneous injection of Endostar, the weight loss would be alleviated and histological examination showed that Endostar alleviated inflammatory cell infiltration and reduced the collagen deposition. These results suggested that Endostar could inhibit the progression of RIPF in mice model.

In 1963, Turner-Warwick M et al. first reported the neovascularization increased in the lungs of patients with IPF [7]. Further evidence strongly suggested that the activation of fibroblast proliferation and accumulation of extracellular matrix (ECM) during the repair process required neovascularization [36-38]. To date, many positive and negative angiogenic were confirmed to modulate angiogenesis process[39]. Among these, VEGF is a major enhancer of vascular permeability which has been widely reported being overexpressed in fibrotic lungs[40]. Armed with this information, inhibition of VEGF in pulmonary fibrosis may have protective effects against angiogenesis and fibrogenesis. In our study, we noted a pronounced decrease in VEGF mRNA expression after Endostar administration. Meanwhile, Endostar significantly attenuated the expression of CD31 which was used to measure angiogenesis. We confirmed the anti-angiogenic efficiency and the down regulation of VEGF expression by Endostar in RIPF. This finding supported the contribution of VEGF to the fibrotic process via angiogenesis induction [41].

Studies on the mechanism of fibrosis show that MFBs are the core effector cells in fibrosis[42]. Continuously activated MFBs can cause excessive deposition of ECM by secreting excess collagen (mainly Collagen I), and the high expression of α -SMA (MFBs marker) can cause excessive contraction of tissue and decreased compliance, which ultimately leads to fibrosis[43-45]. Therefore, MFBs have grown up to be an important target for anti-fibrotic treatment. There are numerous ways to induce the activation of MFBs, among which TGF- β 1 is a key regulator of fibrosis that acts through the activation of MFBs[46]. The increase expression of TGF- β 1 is considered to be one of signs of RIPF[47]. TGF- β 1 induced the activation of MFBs is mainly regulated by Smad3[48], which can be regulated by Ras / MEK / ERK pathway[49]. Our results showed that the expression of α -SMA, TGF- β 1 and Collagen I were significantly increased after 12 and 24 weeks of chest irradiation in mice, which mean the activation of MFBs. The expression level of Smad3 and ERK phosphorylation were significantly elevated as well. The administration of Endostar significantly inhibited the increased protein level of α -SMA, TGF- β 1, p-Smad3 and p-ERK after radiation in lung tissue of mice, indicating Endostar would inhibit the activation of MFBs by suppressing the TGF- β 1/Smad3/ERK pathway, thereby restraining the progression of RIPF.

Conclusion

This study provides evidence that Endostar can effectively inhibit the inflammatory reaction, collagen deposition and abnormal angiogenesis associated with pulmonary fibrosis by inhibiting VEGF and TGF- β 1/Smad3/ERK pathway. Although our study is based on an animal model that cannot fully recapitulate

human RIPF, Endostar presents as a promising agent for RIPF treatment. Further investigation should be explored to in depth understand the specific mechanism of action of Endostar, including elucidating the effector molecules and signal transduction pathways.

Abbreviations

alveolar-capillary barrier	ACB
analysis of variance	ANOVA
α -smooth muscle actin	α -SMA
basic fibroblast growth factor	bFGF
bronchoalveolar lavage fluid	BALF
distal lung epithelial cel	DLEC
extracellular signal-regulated kinase	ERK
enhanced chemiluminescent reagent	ECL
Endostar alone group	EN
extracellular matrix	ECM
epithelial-to-mesenchymal transition	EMT
hematoxylin-eosin	H&E
immunohistochemistry	IHC
idiopathic pulmonary fibrosis	IPF
monocyte chemotactic protein-1	MCP-1
myofibroblasts	MFBs
vinorelbine platinum	NP
no treatment group	NT
non-small cell lung cancer	NSCLC
platelet-derived growth factor	PDGF
reverse transcription-polymerase chain reaction	RT-PCR
radiation-induced lung injury	RILI
radiation alone group	RT
radiation-induced pulmonary fibrosis	RIPF
drosophila mothers against decapentaplegic protein 3	Smad3
transforming growth factor- β 1	TGF- β 1
tumor necrosis factor- α	TNF- α
vascular endothelial growth factor	VEGF

Declarations

(1). Ethics approval and consent to participate

The use of C57BL/6J mice was approved by Animal Care and Use Committee of Zhejiang cancer hospital

(2). Consent for publication

The study was undertaken with the author's consent.

(3). Availability of data and material

Not applicable.

(4). Competing interests

The authors declare that they have no conflicts of interests.

(5). Funding

This work was supported by the National Natural Science Foundation of China (No.81703018, No.81672972), Natural Science Foundation of Zhejiang Province (No.LQ17H180003), and Medical Health Science and Technology Project of Zhejiang Provincial Health Commission (No.2016KYA048-01). National Natural Science Foundation of China are mainly used for the purchase and feeding costs of mice. Natural Science Foundation of Zhejiang Province (No.LQ17H180003) is mainly used for the purchase of reagents, and Medical Health Science and Technology Project of Zhejiang Provincial Health Commission (No.2016KYA048-01) is mainly used for the costs of publication.

(6). Authors' contributions

FM and YHJ designed the study. YHJ performed the statistical analyses and wrote the manuscript. ZC,YHJ,CYM, DBQ and CMY carried out the animal experiments. CM and FM contributed to the study design and to revise critically the manuscript. All the authors read and approved the final version of the manuscript.

(7). Acknowledgements

We thank the staff at Zhejiang Key Laboratory of Radiation Oncology, Zhejiang Cancer Hospital. We also thank Shandong Simcere-Medgenn Bio-Pharmaceutical Co., Ltd. Yantai, China for providing Endostar.

References

1. Han S, Gu F, Lin G, Sun X, Wang Y, Wang Z, et al. Analysis of Clinical and Dosimetric Factors Influencing Radiation-Induced Lung Injury in Patients with Lung Cancer. *J Cancer*. 2015; 6:1172-8.
2. Rajan Radha R, Chandrasekharan G. Pulmonary injury associated with radiation therapy- Assessment, complications and therapeutic targets. *Biomed Pharmacother*. 2017; 89: 1092-104.
3. Yao Y, Zheng Z, Song Q. Mesenchymal stem cells: A double-edged sword in radiation-induced lung injury. *Thorac Cancer*. 2018; 9: 208-17.
4. Giridhar P, Mallick S, Rath GK, Julka PK. Radiation induced lung injury: prediction, assessment and management. *Asian Pac J Cancer Prev*. 2015; 16: 2613-7.
5. [Burdick MD](#), [Murray LA](#), [Keane MP](#), [Xue YY](#), [Zisman DA](#), [Belperio JA](#), et al. CXCL11 attenuates bleomycin-induced pulmonary fibrosis via inhibition of vascular remodeling. *AM J Respir Crit Care Med*. 2005; 171: 261-8.
6. [Hamada N](#), [Kuwano K](#), [Yamada M](#), [Hagimoto N](#), [Hiasa K](#), [Egashira K](#), et al. Anti-vascular endothelial growth factor gene therapy attenuates lung injury and fibrosis in mice. *J Immunol*. 2005; 175:1224-31.
7. Turner-Warwick M. Precapillary systemic pulmonary anastomoses. *Thorax*. 1963; 18: 225-37.
8. [Ackermann M](#), [Kim YO](#), [Wagner WL](#), [Schuppan D](#), [Valenzuela CD](#), [Mentzer SJ](#), et al. Effects of nintedanib on the microvascular architecture in a lung fibrosis mode. *Angiogenesis*. 2017; 20: 359-72.
9. Li X, Yao QY, Liu HC, Jin QW, Xu BL, Zhang SC, et al. Placental growth factor silencing ameliorates liver fibrosis and angiogenesis and inhibits activation of hepatic stellate cells in a murine model of chronic liver disease. *J Cell Mol Med*. 2017; 21: 2370-85.
10. Li Z, Yan H, Yuan J, Cao L, Lin A, Dai H, et al. Pharmacological inhibition of heparin-binding EGF-like growth factor promotes peritoneal angiogenesis in a peritoneal dialysis rat model. *Clin Exp Nephrol*. 2018; 22: 257-65.
11. [O'Reilly MS](#), [Boehm T](#), [Shing Y](#), [Fukai N](#), [Vasios G](#), [Lane WS](#), et al. Endostatin: an endogenous inhibitor of angiogenesis and tumor growth. *Cell*. 1997; 88: 277-85.
12. Boehm T, Folkman J, Browder T, O'Reill MS. Antiangiogenic therapy of experimental cancer does not induce acquired drug resistance. *Nature*. 1997; 390: 404-7.
13. Folkman J. Antiangiogenesis in cancer therapy-endostatin and its mechanisms of action. *Exp Cell Res*. 2006; 312: 594-607.
14. [Herbst RS](#), [Hess KR](#), [Tran HT](#), [Tseng JE](#), [Mullani NA](#), [Charnsangavej C](#), et al. Phase I study of recombinant human endostatin in patients with advanced solid tumors. *J Clin Oncol*. 2002; 20: 3792-803.
15. Thomas JP, Arzoomanian RZ, Alberti D, Marnocha R, Lee F, Friedl A, et al. A Phase I pharmacokinetic and pharmacodynamic study of recombinant human endostatin in patients with advanced solid tumors. *J Clin Oncol*. 2003; 21:223-31.

16. Song HF, Liu XW, Zhang HN, Zhu BZ, Yuan SJ, Liu SY, et al. Pharmacokinetics of His-tag recombinant human endostatin in Rhesus monkeys. *Acta Pharmacol Sin.* 2005; 26:124-8.
17. Jia H, Kling J. China offers alternative gateway for experimental drugs. *Nat Biotechnol.* 2006; 24: 117-8.
18. Wang J, Sun Y, Liu Y, Yu Q, Zhang Y, Li K, et al. Rh-endostatin (YH-16) in combination with vinorelbine and cisplatin for advanced non-small cell lung cancer: a multicenter phase II trial. *Chin New Drug J.* 2005; 14: 204-7.
19. Shi HL, Xu LY, Liu Z. Phase II clinical trial of homemade human rh-endostatin in the treatment of patients with stage IIB-IV non-small cell lung cancer. *Chin J Lung Cancer.* 2004; 7: 325-8.
20. Wang J, Sun Y, Liu Y, Yu Q, Zhang Y, Li K, et al. Results of randomized, multicenter, double-blind phase II trial of rh-endostatin (YH-16) in treatment of advanced non-small cell lung cancer. *Chin J Lung Cancer.* 2005; 8: 283-90.
21. Liu YY. Phase III Clinical Trial of Recombinant Human Endostatin in the Treatment for Advanced Non-small Cell Lung Cancer Patients. *Chin Cancer.* 2005; 14: 398-400.
22. Ling Y, Yang Y, Lu N, You QD, Wang S, Gao Y, et al. Endostar, a novel recombinant human endostatin, exerts antiangiogenic effect via blocking VEGF-induced tyrosine phosphorylation of KDR/Flk-1 of endothelial cells. *Biochem Biophys Res Commun.* 2007; 361: 79-84.
23. Wan YY, Tian GY, Guo HS, Kang YM, Yao ZH, Li XL, et al. Endostatin, an angiogenesis inhibitor, ameliorates bleomycin-induced pulmonary fibrosis in rats. *Respir Res.* 2013; 14: 56.
24. Yamaguchi Y, Takihara T, Chambers RA, Veraldi KL, Larregina AT, Feghali-Bostwick CA. A peptide derived from endostatin ameliorates organ fibrosis. *Sci Transl Med.* 2012; 4: 136-71.
25. Richter AG, McKeown S, Rathinam S, et al. Soluble endostatin is a novel inhibitor of epithelial repair in idiopathic pulmonary fibrosis. *Thorax.* 2009; 64: 156-61.
26. Richter AG, McKeown S, Rathinam S, Harper L, Rajesh P, McAuley DF, et al. Cytokines and radiation-induced pulmonary injuries. *J Radiat Res.* 2018; 59: 709-53.
27. Zhang K, Yang S, Zhu Y, Mo A, Zhang D, Liu L. Protection against acute radiation-induced lung injury: a novel role for the anti-angiogenic agent Endostar. *Mol Med Rep.* 2012; 6: 309-15.
28. Zheng YF, Ge W, Xu HL, Cao DD, Liu L, Ming PP, et al. Endostar enhances the antitumor effects of radiation by affecting energy metabolism and alleviating the tumor microenvironment in a Lewis lung carcinoma mouse model. *Oncol Lett.* 2015; 10: 3067-72.
29. Chen J, Liu DG, Yang G, Kong LJ, Du YJ, Wang HY, et al. Endostar, a novel human recombinant endostatin, attenuates liver fibrosis in CCl₄-induced mice. *Exp Biol Med.* 2014; 239: 998-1006.
30. Ashcroft T, Simpson JM, Timbrell V. Simple method of estimating severity of pulmonary fibrosis on a numerical scale. *J Clin Pathol.* 1988; 41: 467-70.
31. Huang X, Wang X, Xie X, Zeng S, Li Z, Xu X, et al. Kallistatin protects against bleomycin-induced idiopathic pulmonary fibrosis by inhibiting angiogenesis and inflammation. *Am J Transl Res.* 2017;

- 9: 999-1011.
32. Yang L, Wang JW, Tang ZM, Liu XW, Huang J, Li SH, et al. A phase I clinical trial for recombinant human endostatin. *Chin New Drug J.* 2004; 13: 548-53.
 33. Ren HT, Li Y, Wang SD, Han CM. Effects of endostatin pretreatment on fibrosis of human skin fibroblasts and the mechanisms. *Chin J Burns.* 2017; 33: 694-8.
 34. Ren HT, Hu H, Li Y, Jiang HF, Hu XL, Han CM. Endostatin inhibits hypertrophic scarring in a rabbit ear model. *J Zhejiang Univ Sci B.* 2013;14: 224-30.
 35. Nishimoto T, Mlakar L, Takihara T, Feghali-Bostwick C. An endostatin-derived peptide orally exerts anti-fibrotic activity in a murine pulmonary fibrosis model. *Int Immunopharmacol.* 2015; 28: 1102-5.
 36. Selman M, Montaña M, Ramos C, Chapela R. Concentration, biosynthesis and degradation of collagen in idiopathic pulmonary fibrosis. *Thorax.* 1986; 41: 355-9.
 37. Brinckerhoff CE, Matrisian LM. Matrix metalloproteinases: a tail of a frog that became a prince. *Nat Rev Mol Cell Biol.* 2002; 3: 207-14.
 38. Pardo A, Selman M. Idiopathic pulmonary fibrosis: new insights in its pathogenesis. *Int J Biochem Cell Biol.* 2002; 34: 1534-8.
 39. Ribatti D. The crucial role of vascular permeability factor/vascular endothelial growth factor in angiogenesis: a historical review. *Br J Haematol.* 2005; 128: 303-9.
 40. Melincovici CS, Boşca AB, Şuşman S, Mărginean M, Mişu C, Istrate M, et al. Vascular endothelial growth factor (VEGF) - key factor in normal and pathological angiogenesis. *Rom J Morphol Embryol.* 2018; 59: 455-67.
 41. Farkas L, Farkas D, Ask K, Möller A, Gaudie J, Margetts P, et al. VEGF ameliorates pulmonary hypertension through inhibition of endothelial apoptosis in experimental lung fibrosis in rats. *J Clin Invest.* 2009; 119: 1298-311.
 42. Abraham DJ, Eckes B, Rajkumar V, Krieg T. New developments in fibroblast and myofibroblast biology: implications for fibrosis and scleroderma. *Curr Rheumatol Rep.* 2007;9:136-43.
 43. Yarnold J, Brotons MC. Pathogenetic mechanisms in radiation fibrosis. *Radiother Oncol.* 2010; 97:149-61.
 44. Friedman SL. Mechanisms of hepatic fibrogenesis. *Gastroenterology.* 2008;134:1655-69.
 45. Barnes JL, Gorin Y. Myofibroblast Differentiation During Fibrosis: Role of NAD(P)H Oxidases. *Kidney Int.* 2011;79: 944-56.
 46. Klingberg F, Chow ML, Koehler A, Boo S, Buscemi L, Quinn TM, et al. Prestress in the extracellular matrix sensitizes latent TGF- β 1 for activation. *J Cell Biol.* 2014; 207: 283-97.
 47. Dadrich M, Nicolay NH, Flechsig P, Bickelhaupt S, Hoeltgen L, Roeder F, et al. Combined inhibition of TGF- β and PDGF signaling attenuates radiation-induced pulmonary fibrosis. *Oncoimmunology.* 2015;5: e1123366.

48. Reisdorf P, Lawrence DA, Sivan V, Klising E, Martin MT. Alteration of transforming growth factor-beta1 response involves down-regulation of Smad3 signaling in myofibroblasts from skin fibrosis. *Am J Pathol.* 2001;159:263-72.
49. Hayashida T, Decaestecker M, Schnaper HW. Cross-talk between ERK MAP kinase and Smad signaling pathways enhances TGF-beta-dependent responses in human mesangial cells. *FASEB J.* 2003;17:1576-8.

Figures

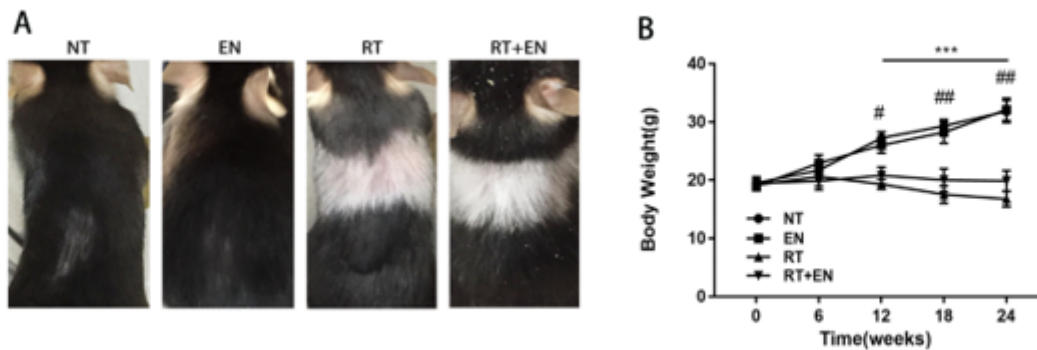


Figure 1

Physical Status. A. The hair of mice in NT and EN groups remained black and glossy, whereas the hair of mice in RT and RT+EN group turned white and dull at six weeks post-irradiation. B. Body weight of each mouse was continuously measured and recorded weekly from week 0 to week 24 (***P*<0.001, RT group compared with NT group, # *P*<0.05, ## *P*<0.01, RT group compared with RT+EN group).

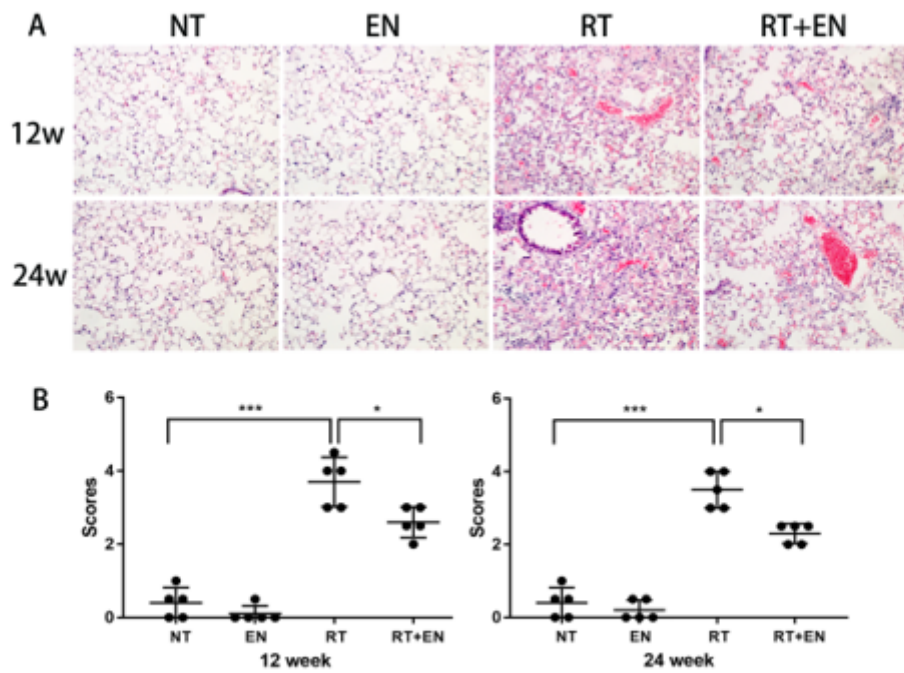


Figure 2

HE staining of lung tissue in the different treatment groups at 12 weeks and 24 weeks. A. No significant histopathologic changes were observed in lung tissue from NT and EN treatment groups. Significant histopathologic changes were observed in lung tissue from RT treatment group, including infiltration of inflammatory cells and destruction of alveolar structure. This inflammatory cells infiltration and destruction of alveolar structure was significantly reduced in RT+EN treatment group.

(Magnification:×200) B. Pneumonitis/alveolitis scores of lung tissue. (n=5,*P<0.05,***P< 0.001)

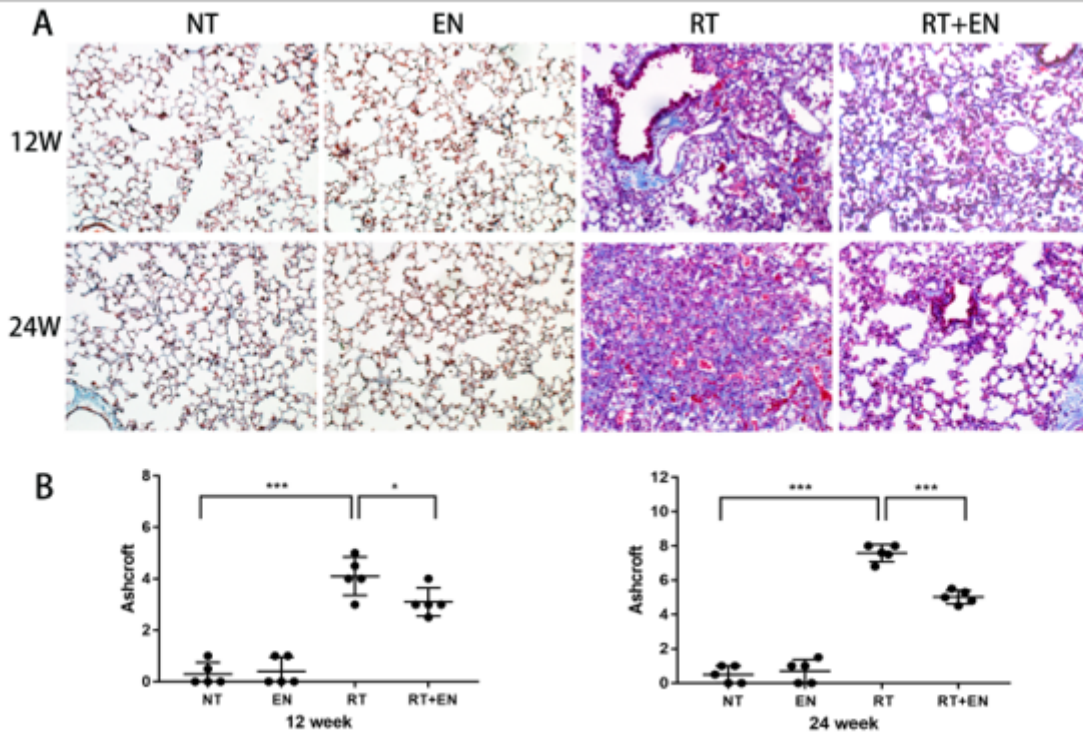


Figure 3

Masson's trichrome staining of lung tissue in the different treatment groups at 12 weeks and 24 weeks. A. In NT and EN treatment groups, the lung tissue fibers exhibited thin and light staining, and the lung tissue structures were normal. Masson's trichrome staining of lung tissue in RT group indicated collagen deposition, alveolar wall destruction and fibrotic areas. RT+EN treatment group displayed significantly reduced collagen deposition and fibrotic lesions compared with RT group (Magnification:×200). B. Fibrosis scores for grading lung histopathological changes (n=5,*P<0.05,**P<0.01,***P< 0.001).

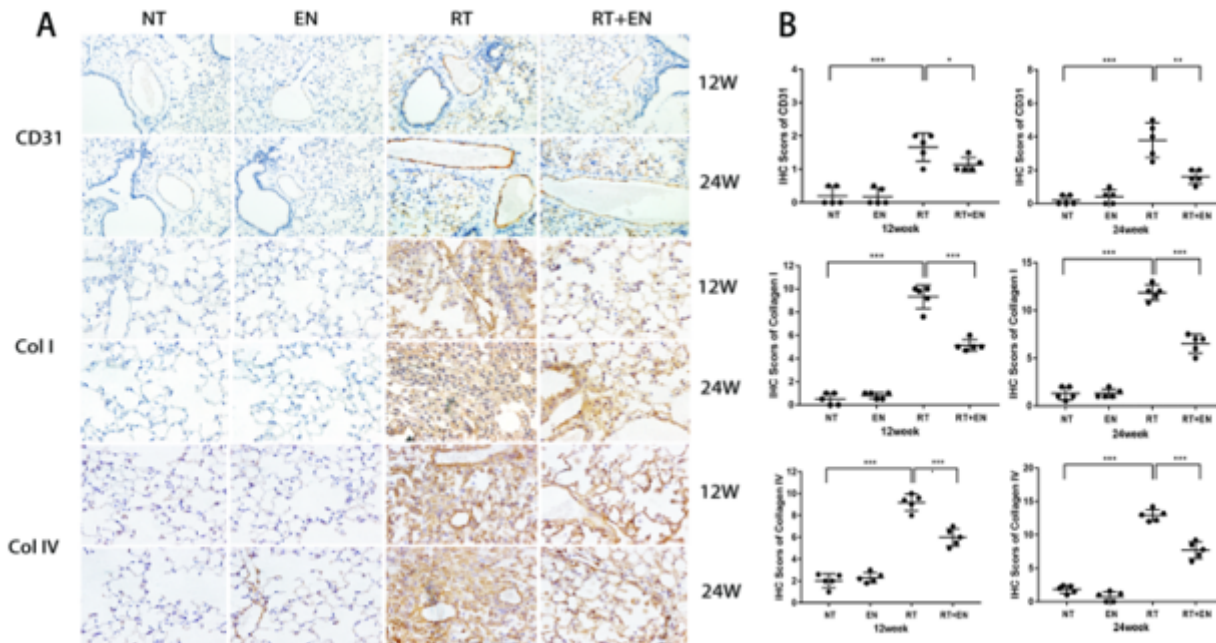


Figure 4

Endostar reduced collagen deposition and angiogenesis in lung tissue induced by radiation. A. The expression of CD31, Collagen I and Collagen IV of lung tissue sections based on IHC. B. Responding IHC scores of lung tissue sections based on IHC (n=5,*P<0.05,**P<0.01,***P< 0.001).

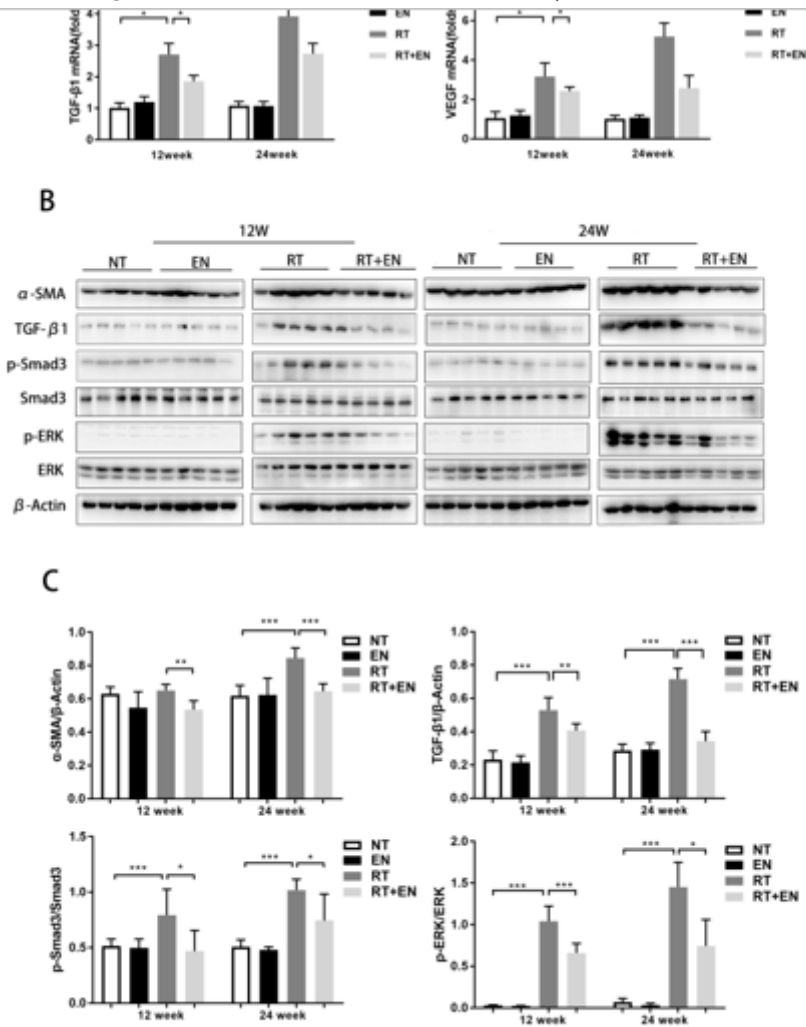


Figure 5

Endostar decreased TGF-β1, VEGF mRNA expression and suppressed myofibroblasts (MFBs) activation by inhibiting TGF-β1/Smad3/ERK pathway in lung tissue of mice after radiation. A. The expression of TGF-β1 and VEGF mRNA levels in mice lung tissues of four different groups by RT-PCR analysis (*P<0.05, **P<0.01). B. Western blot showed the expression of α-SMA, TGF-β1, p-Smad3, Smad3, p-ERK, ERK, β-Actin proteins in lung tissue of four different groups. C. The protein band density analyzed by imageJ software, and the results presented as ratio (n=5, *p<0.05,**p<0.01, ***P<0.001).

Supplementary Files

This is a list of supplementary files associated with this preprint. Click to download.

- [Table1.pdf](#)